Available online at www.sciencedirect.com

ScienceDirect

Energy Procedia 124 (2017) 621–627

Energy Procedia

www.elsevier.com/locate/procedia

7th International Conference on Silicon Photovoltaics, SiliconPV 2017

Crystalline silicon solar cell with front and rear polysilicon passivated contacts as bottom cell for hybrid tandems

Stefan L. Luxembourg[a]*, Dong Zhang[b], Yu Wu[a], Mehrdad Najafi[b], Valerio Zardetto[c], Wiljan Verhees[b], Antonius R. Burgers[a], Sjoerd Veenstra[b], L.J. Geerligs[a]

[a]*ECN Solar Energy, P.O. Box 1, NL-1755 ZG Petten, The Netherlands*
[b]*ECN-Solliance, High Tech Campus 21, NL-5656 AE Eindhoven, The Netherlands*
[c]*TNO-Solliance, High Tech Campus 21, NL-5656 AE Eindhoven, The Netherlands*

Abstract

In this paper we analyze and model perovskite/c-Si tandem cells with front and rear polySi passivated contacts on the bottom cell. A high-efficiency tandem approach will benefit from the high V_{oc} potential of a c-Si bottom cell with front and rear polySi passivated contacts while the combination with a high band gap, semi-transparent, perovskite top cell will largely diminish the UV-Vis parasitic absorption in a polySi front side layer on the c-Si cell. On the other hand since the J_{sc} is strongly reduced in a tandem bottom cell, free carrier absorption, to which both front and rear polySi layers contribute, will become a relatively more important loss mechanism. We investigate the trade-off between the optical gains and resistive losses from reducing the polySi thickness for cell configurations without transparent conductive oxide (TCO) and also consider the potential of the combination with TCOs. From our optical simulations we conclude that optical losses in the polySi layers of 100 nm and below are limited when applied on the bottom cell. Taking into account resistive losses in the polySi layers of varying thickness the optimal thickness is found to be 50 nm. In combination with the high V_{oc} values resulting from the application of polySi passivating contacts this offers a promising route to establish a bottom cell with high efficiency. The combination of very thin polySi with highly transparent TCOs is likely to further improve bottom cell performance.

Peer review by the scientific conference committee of SiliconPV 2017 under responsibility of PSE AG.

Keywords: Passivating contacts; Polysilicon; ray-tracing; Multijunction; Tandem; Perovskite solar cell

* Corresponding author. Tel.: +31-88-515-8256; fax: +31-88-515-8214.
E-mail address: luxembourg@ecn.nl

1876-6102
Peer review by the scientific conference committee of SiliconPV 2017 under responsibility of PSE AG.
10.1016/j.egypro.2017.09.091

1. Introduction

Polysilicon (polySi) passivated contacts [1,2] hold great potential for the large scale implementation of the concept of highly carrier selective contacts in industrial crystalline silicon (c-Si) solar cells. In comparison to amorphous silicon based carrier selective contacts their compatibility with high-temperature screen-printed metallization is attractive. Recently, we have demonstrated 21.3% efficiency with the bifacial Passivated Emitter and Rear Polysilicon cell design, which combines a diffused front side emitter with an n++ doped polySi rear contact, with fire-through (FT) metallization grids [3,4]. In such a cell structure performance is limited by front surface recombination. However, while the implementation of front side polySi contacts would reduce front surface recombination, it would also introduce significant UV-Vis parasitic absorption. It has been shown that in order to limit the J_{sc} losses to 1 mA/cm^2 under AM 1.5 illumination a front side polySi thickness should not exceed 20 nm [5]. For these low polySi layer thicknesses and their accompanying high sheet resistances (R_{sheet}) it is required to combine the polySi layer with a transparent conductive oxide (TCO) for lateral carrier transport, which by itself will induce parasitic absorption losses as well.

In a tandem configuration with a high band gap, semi-transparent, perovskite top cell the UV-Vis parasitic absorption in a polySi front side layer on a c-Si cell will be largely diminished. Moreover, a high efficiency tandem approach will also benefit from the high V_{oc} potential of a c-Si bottom cell with front and rear polySi passivated contacts. In comparison to heterojunction devices which are often employed as bottom cell in a high efficiency hybrid tandem strategy the front-and-rear-polySi cells are compatible with industrial high temperature diffusion and screen-printed metallization steps. On the other hand, free carrier absorption (FCA) of near-infrared photons needs attention in polySi layers in general, and in particular in such c-Si bottom cells with dual polySi contact layers: the J_{sc} is strongly reduced in a tandem bottom cell, so that the FCA, to which both front and rear polySi layers contribute, becomes a relatively more important loss mechanism than in a single junction (SJ) c-Si cell.

In this paper we analyze and model perovskite/c-Si tandem cells with front and rear polySi passivated contacts on the bottom cell. Focus is on the analysis of optical losses in the polySi layers: the UV-Vis absorption and the FCA. We investigate the trade-off between the optical gains and resistive losses from reducing the polySi thickness, for cells where the polySi layers are applied on their own (without additional layers for lateral conductance), and indicate the effect of combing the polySi layers with a TCO layer. The optical losses of front-and-rear-polySi cells as bottom cells are compared to that of an n-PERT cell fabricated with industrial processes. We use optical ray-tracing simulations combined with detailed optical and electrical measurements of the cells and individual layers.

2. Materials and methods

The semi-transparent perovskite solar cell (PSC) used as top cell in this study includes a triple-cation perovskite absorber material with a band gap of 1.55 eV. This organic-inorganic trihalide perovskite material, with general formulation APbX3 (X is a halide), consists of a mixture of methylammonium (CH_3NH_3, MA), formamidinium ($HC(NH_2)_2$, FA) and Cs A-site cations which offers enhanced thermal stability and band gap tuning possibilities over the MA tri-iodide absorber [6]. The p-i-n top cell structure with the triple-cation perovskite ($Cs_{0.05}(MA_{0.17}FA_{0.83})_{0.95}Pb(I_{0.9}Br_{0.1})_3$) is shown in Fig. 1a. It includes a 770 nm thick absorber layer and a highly transparent NiO_x hole transport layer. More details will be included in a forthcoming publication.

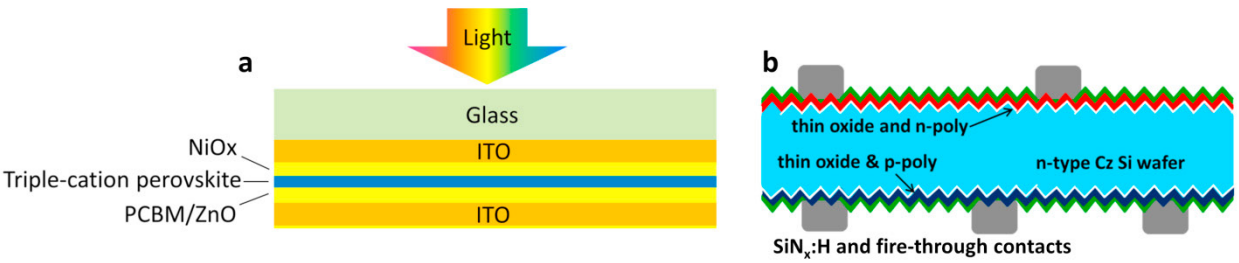

Fig. 1. (a) Structure of a semi-transparent perovskite top cell; (b) bifacial c-Si solar cell with front and rear polySi passivated contacts with front and rear SiN_x coating and FT metallization.

Front-and-rear-polySi solar cells were fabricated on n-type Cz wafers with symmetric in-situ doped p-poly depositions by a Tempress low pressure chemical vapour deposition (LPCVD) system, followed by overcompensation into n-poly by implanting phosphorus on one side, and activation anneal. Plasma enhanced chemical vapour deposited (PECVD) SiN_x:H coating was deposited on both sides, which importantly provides hydrogenation of the polySi contact layer. Firing-through contact grids were directly screen printed on the cells capped with SiNx:H, using standard n-type Si contacting Ag paste on n-polySi and p-type Si contacting Ag/Al paste on p-polySi, followed by firing. For more details the reader is referred to [7]. Cell performance was characterized by I-V measurement (Wacom class AAA steady state solar simulator). Low-injection level I-V measurements (mimicking bottom cell illumination conditions) were realized using grey filters.

Ray-tracing simulations of the complete tandem stack were performed using the GenPro4 optical simulation software developed at Delft University of Technology [8]. Zhang *et al.* have used this model in the past to simulate 4-terminal (4-T) hybrid tandem structures with a methylammonium tri-iodide perovskite top cell and a MWT (n-PERT) bottom cell [9]. For the present study the top cell was replaced by the semi-transparent PSC in Fig. 1a. As bottom cell we implemented the front-and-rear-polySi contacts solar cell, as depicted in Fig. 1b, in the model. To model the 4-T tandem configuration the bottom cell was encapsulated in EVA and combined with a reflective backsheet.

Optical data of all materials in the PSC layer stack were obtained from spectroscopic ellipsometry (SE). For SE all individual layers were prepared on Corning glass. SE as well as Reflection-Transmission (R/T) spectroscopy were performed on an approximately 100 nm thick n-type polySi sample with phosphorus doping concentration of 3×10^{20} cm^{-3} on a mechanically polished Cz wafer with 100 nm thermal oxide. The optical properties of the (rear) p-type polySi material were not studied in detail yet. Since the p-polySi is positioned at the rear of the cell only the wavelength range > 1000 nm is of importance. We have assumed that in this spectral range it can be well described using c-Si optical data [10] with c-Si parameterization of the FCA [11] (see next section for more details).

3. Results

The JV-characteristics of the semi-transparent triple-cation Perovskite top cell are included in Table 1. The measurements showed low hysteresis, and a stabilized efficiency of 14.7% was realized in a five minute maximum power point tracking experiment. Preconditioning by a 10 minute UV exposure from the glass side was applied. The current top cell design allows further (optical) optimization which will be detailed in a forthcoming publication.

Table 1. Overview of JV characteristics of the solar cells discussed in the main text. *) entries were obtained from bottom cell injection level grey filter measurements, **) entry was obtained from optical modelling. F & R stands for front-and-rear.

Cell	J_{sc} (mA/cm^2)	V_{oc} (V)	FF	η (%)
Perovskite top cell	19.7	1.019	0.73	14.6 (14.7 stabilized)
SJ F & R polySi cell	32.0	0.673	0.723	16.0
F & R poly Si bottom cell	12.9**	0.648*	0.743*	6.2
4-T Tandem with poly				20.9

For the n-type polySi material the n, k data derived from SE and R/T spectroscopy can accurately describe the experimental R/T spectrum (data not shown). In comparison to c-Si the polySi material displays significantly higher absorption in the UV-Vis spectral range, as was described before [12]. The NIR absorption closely follows the FCA parameterization of c-Si by Baker-Finch *et al.* [11]. Similar observations were made before by Reiter *et al.* [5]. Since the p-type polySi material is positioned at the rear of the cell considered in this study (see Fig. 1b), only the wavelength range > 1000 nm is of importance. We have assumed that in this spectral range, as for the n-type material, it can be well described using the c-Si optical parameters [10] with the aforementioned FCA parameterization. In the future we intend to undertake further optical studies on polySi which will also include p-type material.

The absorption in the c-Si absorber as obtained from the ray-tracing simulations of the front-and-rear-polySi SJ cell of Fig. 1b was compared to the experimentally derived EQE of this same cell with FT contacts. In this analysis

the absorption in the polySi material is considered to be fully parasitic. The cell had front and rear polySi contacts of 200 nm thickness. The front n-type contact had a R_{Sheet} of 70 Ω/sq and an activated P concentration (from ECV) of 3 × 10^{20} cm^{-3}, the rear p-type polySi contact had an activated B concentration of 3 × 10^{19} cm^{-3}. The measured and simulated EQEs are largely in accordance as can be observed from Fig. 2a. The JV-characteristics of the cell as SJ device are included in Table 1. The V_{oc} of the 200 nm polySi cell was 673 mV, on half-fabricates before metallization an implied V_{oc} of 701 mV was obtained. The doping concentration of the p-polySi in this cell is lower than that of an industrial diffused emitter. Recently, we have realized implied V_{oc} values up to 713 mV on half fabricates with a higher B concentration of 1 × 10^{20}, and by employing a polished rear side surface of the wafer, implied V_{oc} values of about 730 mV will be feasible [13].

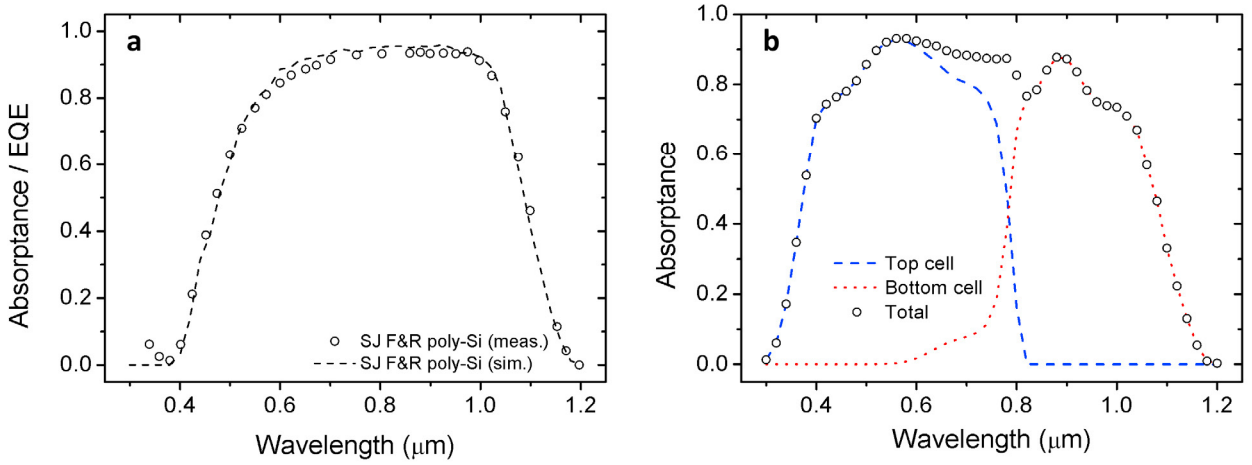

Fig. 2. (a) Comparison of the measured EQE spectrum of the F & R polySi cell of Fig. 1b and the absorptance of the c-Si bulk wafer obtained from the optical simulation of the cell; (b) Simulated top and bottom cells' EQEs.

In order to estimate the performance of the front-and-rear-polySi cell as bottom cell, we used the ray-tracing model to simulate the performance of the full tandem stack with the triple-cation perovskite top cell. The full stack includes the perovskite top cell as shown in Fig. 1a and the bottom cell encapsulated with EVA. Fig. 2b shows the simulated absorption in the top and bottom cell absorber layers. From this analysis a J_{sc} of 12.9 mA/cm^2 was derived for the bottom cell (including shading losses). To get to an estimate of the 4-T performance V_{oc} and FF parameters were derived from JV measurements using a set of grey filters. From this analysis the bottom cell efficiency was found to be 6.2% and the 4-T efficiency 20.9%. The data is included in Table 1.

The effect of the thickness of the front and rear polySi layers on the maximum J_{sc} implemented as bottom cell in the described tandem stack was studied using the optical model. As the B-concentration of the experimental device (3 × 10^{19} cm^{-3}) results in very high R_{sheet} values, we assumed a more heavily doped polySi (1 × 10^{20} cm^{-3}) layer in our simulations. The experimentally obtained R_{Sheet} for this doping concentration was 265 Ω/sq. ΔJ_{sc} for the cells with front and rear polySi thickness *d* was derived from a comparison of the absorption in the c-Si absorber layer for this structure and for a c-Si wafer with just 80 nm SiN_x on front and rear. In this analysis the effect of front metal grid shading is not taken into account (active area only). Fig. 3a includes the results of two analyses: 1) front and rear polySi thickness were changed equally; 2) only the front polySi thickness was changed while the rear polySi thickness was kept at 200 nm. The parasitic absorption in the polySi layers is dominated by FCA. For the 200 nm front-and-rear-polySi cell a total parasitic absorption of is 1.5 mA/cm^2 found, of which 0.4 mA/cm^2 corresponds to absorption below 1000 nm (in the front polySi layer). In absence of the polySi layers an active area J_{sc} of 15.5 mA/cm^2 was derived. For comparison, we have included the FCA J_{sc} loss for an n-PERT cell (horizontal dashed line), also obtained from ray-tracing simulations.

Clearly, as is the case for the SJ application of front-and-rear-polySi cells a reduction of the polySi layer thickness results in a significant reduction in parasitic absorption, which for 200 nm thick polySi layers amounts to

approximately 10% of the total J_{sc} of the cell in tandem application. For a front and rear polySi thickness of 75 nm the estimated current loss is close to the estimated FCA losses for the n-PERT cell. Thus, the simulations indicate that for a thickness of 75 nm and lower the optical losses in polySi can be reduced to the level of diffused cells. Therefore, with the advantage of the possible high V_{oc} values of the front-and-rear-polySi cells, these cells can potentially outperform diffused cells as bottom cell in a hybrid tandem stack. However, since the carrier mobility in polySi is reduced relative to c-Si, the resistive losses in thin polySi layers will be more severe than in diffused junctions and this needs to be considered in the analysis of this tandem concept. Here, we note that in comparison to SJ operation the current densities are relatively low. In addition to the resistive losses there are also practical considerations that may pose a lower limit to the polySi thickness: FT metallization on very thin polySi layers may result in large contact recombination values. Nevertheless, recently we obtained for 100 nm thin polySi layers estimated $j_{0,\,metal}$ values of 100 – 200 fA/cm^2 for fire-through metallization [4].

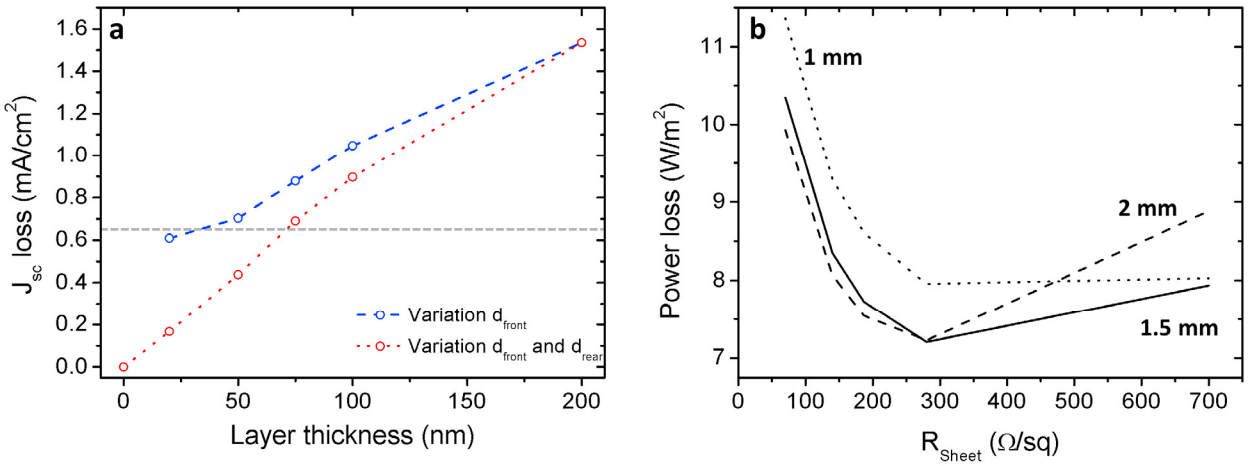

Fig. 3. (a) Short circuit current density loss as function of the polySi thickness; (b) Power loss calculated as function of R_{Sheet} for three different finger pitches.

In order to obtain a more detailed understanding of the effect thinner polySi contact regions will have on the cell performance, we have performed a power loss analysis. The following factors have been included in this analysis: 1) shading losses from metal fingers at front, 2) FCA by the doped polySi layers, 3) polySi resistive losses. The analysis was performed for several finger pitches and a fixed finger width of 50 µm and varying either both front and rear polySi thicknesses or just the front polySi thickness. In the analysis we used the JV-parameters of the cell detailed above with 200 nm polySi thickness and FT metallization (see also Table 1). In our experience, the R_{sheet} of the polySi often scales roughly inversely with the thickness, so this was assumed in the calculations. The resistive power loss was calculated according to [14]. The power losses due to shading and FCA were calculated using V_{mp} corrected for the resistive losses. The results of the power loss analysis for a varying front n-poly thickness and a constant rear p-polySi thickness of 200 nm are included in Fig. 3b. For decreasing layer thickness (increasing R_{Sheet} along the x-axis) there is at first a strong decrease in the power loss due to reduction in parasitic absorption losses, then the reduction saturates due to increasing resistive losses, and eventually the increasing resistive losses make the total power loss increase again. The Fig. also illustrates the effect of the finger pitch: for small pitch the resistive loss has less of an effect, while on the other hand relatively large optical losses for the lower R_{Sheet} values are present.

This power loss analysis indicates that the optimal n-polySi R_{Sheet} is between 200 and 300 Ω/sq, corresponding to a polySi thicknesses of 50 nm. We should note that FT metallization of such thin polySi layers with low contact recombination has not been demonstrated as yet. For very thin polySi layers (10 - 20 nm) the resistive losses will dominate and deteriorate the performance, hence, for these thicknesses a combination with TCO layers should be used to result in sufficient lateral conductivity. While TCO materials like ITO also induce significant parasitic FCA,

application of highly transparent TCO's like In_2O_3:H or ZnO:H in such a layer stack can reduce the overall losses. As can observed from Fig. 3a, when the parasitic losses in TCO can be fully neglected, such a layer stack could result in an increase of J_{sc} of at most 0.4 mA/cm^2, which corresponds to approximately 2 W/m^2, compared to application of a stand-alone polySi layer of 50 nm. Additionally, the resistive losses in the 50 nm thin polySi which are estimated to be around 2 W/m^2 can be significantly reduced by application of a stack of very thin polySi with highly transparent, highly conductive, TCO.

4. Conclusions

We have shown that when applied as bottom cell with a high band gap perovskite top cell, UV-Vis parasitic absorption in a polySi passivated contact layer on the front of a c-Si cell is largely prevented. Nevertheless, for a cell with 200 nm thick front and rear polySi layers, performance is still limited by the mainly long wavelength optical losses (free carrier absorption). Reduction of the polySi thickness is a viable option to improve the performance. The optimal front polySi layer thickness is derived from a power loss analysis to be 50 nm, for the polySi layer characteristics (doping level, carrier mobility) of our polySi process. The combination of highly transparent TCOs like In_2O_3:H or ZnO:H with very thin polySi layers will further reduce optical and resistive losses. Currently, compatibility with fire-through metallization has been demonstrated down to 100 nm polySi thickness. Our optical simulations indicate that at this thickness the J_{sc} loss compared to a totally diffused cell is limited (about 0.25 mA/cm^2) in combination with the gains in V_{oc} from the application of the polySi passivating contacts this offers a promising route to establish a high efficiency bottom cell.

Acknowledgements

The authors would like to acknowledge Dr. Rudi Santbergen, Delft University of Technology, for the analysis of the n-type polySi material by spectroscopic ellipsometry.

References

[1] Glunz SW, Feldmann F, Richter A, Bivour M, Reichel C, Steinkemper H, Benick J, Hermle M. The Irresistible Charm of a Simple Current Flow Pattern – 25% with a Solar Cell Featuring a Full-Area Back Contact. Proceedings of the 31st EU-PVSEC, pp. 259-263 (2015).

[2] Römer U, Peibst R, Ohrdes T, Lim B, Krügener J, Wietler T, Brendel R. Ion implantation for poly-Si passivated back-junction back-contacted solar cells IEEE J. Photovolt. 2015;5:507-514.

[3] Stodolny MK, Lenes M, Wu Y, Janssen GJM, Romijn I, Luchies JRM, Geerligs LJ. N-Type polysilicon passivating contact for industrial bifacial n-type solar cells, Solar Energy Materials and Solar Cells 2016;158:24-28

[4] Stodolny MK, Geerligs LJ, Janssen GJM, van de Loo BWH, Melskens J, Santbergen R, Isabella O, Schmitz J, Lenes M, Luchies J-M, Kessels WMM, Romijn I. Material Properties of LPCVD Processed n-type Polysilicon Passivating Contacts and its Application in PERPoly Industrial Bifacial Solar Cells, presented at the 7th SiliconPV conference Freiburg, submitted to Energy Procedia 2017.

[5] Reiter S, Koper N, Reineke-Koch R, Larionova Y, Turcu M, Krügener J, Tetzlaff D, Wietler T, Höhne U, Kähler J-D, Brendel R, Peibst R. Parasitic absorption in polycrystalline Si-layers for carrier-selective front junctions, Energy Procedia 2016;92:199-204.

[6] McMeekin DP, Sadoughi G, Rehman W, Eperon GE, Saliba M, Hörantner MT, Haghighirad A, Sakai N, Korte L, Rech B, Johnston MB, Herz LM, Snaith HJ. A mixed-cation lead mixed-halide perovskite absorber for tandem solar cells, Science 2016;351:151-155

[7] Wu Y, Stodolny MK, Geerligs LJ, Lenes M, Luchies J-M. In-situ doping and local overcompensation of high performance LPCVD polysilicon passivated contacts as approach to industrial IBC cells, Energy Procedia 2016;92:427-433.

[8] Santbergen, R, Mishima R, Meguro T, Hino M, Uzo H, Blanker J, Yamamoto K, Zeman M. Minimizing optical losses in monolithic perovskite/c-Si tandem solar cells with a flat top cell, Optics Express 2016;24:1288-1299.

[9] Zhang D, Verhees W, Dörenkamper M, Qui W, Bakker K, Gutjahr A, Veenstra S, Gehlhaar R, Paetzold, UW, Soppe W, Romijn I, Geerligs, LJ, Aernouts T, Weeber A. Combination of Advanced Optical Modelling with Electrical Simulation for Performance Evaluation of Practical 4-terminal Perovskite/c-Si Tandem Modules, Energy Procedia 2016;92:669-677

[10] Green M. Self-consistent optical parameters of intrinsic silicon at 300K including temperature coefficients, Solar Energy Materials & Solar Cells 2008;92:1305–1310.

[11] Baker-Finch SC, McIntosh KR, Yan D, Fong KC, Kho TC. Near-infrared free carrier absorption in heavily doped silicon, J. App. Phys. 2014;116:063106.

[12] Feldmann F, Reichel C, Müller R, Hermle M. The application of polySi/SiO_x contacts as passivated top/rear contacts in Si solar cells, Sol. Energ. Mat. Sol. Cells 2017;159:265-271.

[13] Ciftpinar HE, Stodolny MK, Wu Y, Janssen GJM, Loffler J, Schmitz J, Lenes M, Luchies JM, Geerligs LJ. Study of Screen Printed Metallization for Polysilicon Passivating Contacts, presented at the 7th SiliconPV conference Freiburg, submitted to Energy Procedia 2017.
[14] http://pveducation.org/pvcdrom/design/emitter-resistance